

# Experiencing the communication advantage of the Superposition of Causal Orders

Daniele Cuomo

Department of Physics “Ettore Pancini”  
University of Naples Federico II  
daniele.cuomo@unina.it

Marcello Caleffi

*IEEE Senior member*  
Department of Electrical Engineering  
and Information Technology  
University of Naples Federico II  
marcello.caleffi@unina.it

Angela Sara Cacciapuoti

*IEEE Senior member*  
Department of Electrical Engineering  
and Information Technology  
University of Naples Federico II  
angelasara.cacciapuoti@unina.it

**Abstract**—Many recent studies deal with the Superposition of Causal Orders, a quantum operation with promising advantages in both communication or computing. To experience the advantages, there are several way of implementing it. In literature, most of the set-ups are photonic-based. Instead, our interest is witnessing the Superposition of Causal Orders within a programmable technology, based on superconductors. To do that, we focus on a specific case of the subject operation, which could be useful for the future of quantum communication.

**Index Terms**—Superposition of Causal Orders, Quantum Operations, Quantum Circuits, Quantum Communication, Quantum Noise.

## I. INTRODUCTION

The *Superposition of Causal Orders* (SoCO) is an interesting property of quantum mechanics. In brief, it is a quantum evolution where two or more operations occur, but the space-time order in which they occur is causally ordered by an extra quantum system. This creates a superposition of causal orders among those operations. The SoCO has practical implications: from a communication perspective, noisy channels are superposed in order to increase the overall capacity [1]–[3], whereas, in the computing paradigm, it is a way to define discrimination predicates [4], [5].

There are several way to physically implement a superposition of orders. Most of realizations are photonic-based [6]–[10], but it is not the only way. Indeed, within this paper we present an implementation of the SoCO with a programmable technology, based on superconductors [11], [12].

Whenever the SoCO implementation requests that the information carrier is subject to each operation only once, that implementation is called a *quantum switch* [13]. The quantum switch is an optimal implementation of the SoCO, in terms of *query complexity*<sup>1</sup>. Any other implementation has a sub-optimal query complexity. However, many available technologies are based on the *standard circuit model* [14]. For this reason, only sub-optimal implementations are possible meeting that model.

The aim of this paper is experiencing and evaluating the SoCO within a *Noisy Intermediate-Scale Quantum* (NISQ)

architecture [15], based on superconductors. NISQ architectures are widespread and they promise to be resources of practical interest in the next future. Furthermore, their design is likely to rapidly evolve, also by considering the SoCO as resource. Our hope is to enrich the knowledge on the capabilities of current quantum technologies, with the long-term goal of contributing to shape future architecture designs.

The experiment set-up is meant to witness the communication advantage, resulting from a specific case of the SoCO. In the communication paradigm, operations model noisy channels affecting quantum information. According to *quantum Shannon theory* [16], the capacity is a metric to quantify the ability for a noisy channel to convey quantum information, without destroying it. A channel with null capacity totally destroys the *coherence* of the quantum information. By superposing two or more null capacity channels, the result is a new channel that is a SoCO. That new channel has a not-null capacity, an interesting behaviour from a practical point of view [2], [3].

## II. PRELIMINARIES

### A. Density matrices and operations

To our purpose – modeling noisy channels – using the ket notation formalism is not enough. A more general way of describing quantum states is with density matrices. Accordingly, any state  $|\varphi\rangle$  is said to be *pure* and it is described by the density matrix  $\rho = |\varphi\rangle\langle\varphi|$ . The formalism also considers *mixture* of pure states, i.e., a density matrix  $\rho = \sum_i p_i |\varphi_i\rangle\langle\varphi_i|$ , with  $\{p_i\}_i$  being a normalized set of probabilities.

Let  $\mathcal{N} : \mathbb{H} \rightarrow \mathbb{H}$  be an operation modeling a noisy channel acting on a quantum information  $\rho$ . Therefore,  $\mathbb{H}$  is the space spanned by  $\{|\varphi_i\rangle\langle\varphi_i|\}_i$ . Its effects on  $\rho$  can be expressed through the operator-sum representation as follows [17]:

$$\mathcal{N}(\rho) = \sum_i N_i \rho N_i^\dagger \quad (1)$$

where  $\{N_i\}_i$  are called Kraus operators and it holds  $\sum_i N_i^\dagger N_i = \mathbb{1}$ , with  $\mathbb{1}$  being the identity matrix.

<sup>1</sup>The number of time a primitive operation occurs.

If we consider two operations  $\mathcal{N}$  and  $\tilde{\mathcal{N}}$ , both acting on  $\rho$  in a well-definite order, say  $\mathcal{N}$  first and  $\tilde{\mathcal{N}}$  second, the overall operation is described by the composition function:

$$(\tilde{\mathcal{N}} \circ \mathcal{N})(\rho) = \sum_{ij} \tilde{N}_j N_i \rho N_i^\dagger \tilde{N}_j^\dagger, \quad (2)$$

where  $\tilde{\mathcal{N}}(\rho) = \sum_j \tilde{N}_j \rho \tilde{N}_j^\dagger$ .

### B. SoCO between two operations

As already mentioned, the SoCO acts on a quantum state by superposing the causal order of two or more operations. Here, we consider the case of two generic operations. After that we fix the operations to model the bit-flip and the phase-flip noise channels, introduced later.

The SoCO of two operations  $\mathcal{N}$  and  $\tilde{\mathcal{N}}$ , is given by [13]:

$$\mathcal{S}_{\rho_c, \mathcal{N}, \tilde{\mathcal{N}}}(\rho) = \sum_{ij} S_{ij}(\rho \otimes \rho_c) S_{ij}^\dagger, \quad (3)$$

where  $\rho_c \triangleq |\varphi_c\rangle \langle \varphi_c|$  is a *control state* and  $\{S_{ij}\}_{ij}$  denotes the set of Kraus operators given by  $S_{ij} = N_i \tilde{N}_j \otimes |0\rangle \langle 0| + \tilde{N}_j N_i \otimes |1\rangle \langle 1|$ .

As assumed in [2], in the following we consider two operations  $\mathcal{N}$  and  $\tilde{\mathcal{N}}$  modeling the *bit-flip* and the *phase-flip* channels, respectively. Therefore, the Kraus operators describing  $\mathcal{N}$  are<sup>2</sup>  $N_1 = \sqrt{1-p}\mathbb{I}$  and  $N_2 = \sqrt{p}X$ . Similarly, the Kraus operators describing  $\tilde{\mathcal{N}}$  are  $\tilde{N}_1 = \sqrt{1-q}\mathbb{I}$  and  $\tilde{N}_2 = \sqrt{q}Z$ , with  $p$  and  $q$  being classical probabilities.

Ultimately, as a visual reminder, we use  $\mathcal{X}_p$  instead of  $\mathcal{N}$  and  $\mathcal{Z}_q$  instead of  $\tilde{\mathcal{N}}$ . In light of the above, we can model the bit-flip and the phase-flip channels respectively as

$$\mathcal{X}_p(\rho) = \bar{p}\mathbb{I}\rho\mathbb{I} + pX\rho X \quad (4)$$

$$\mathcal{Z}_q(\rho) = \bar{q}\mathbb{I}\rho\mathbb{I} + qZ\rho Z, \quad (5)$$

with  $\bar{p} \triangleq 1-p$  and  $\bar{q} \triangleq 1-q$ .

The last assumption is that the control state is fixed to  $\rho_c = \rho_c^+ \triangleq |+\rangle \langle +|$ . It is possible to show that equation (3) simplifies to

$$\mathcal{S}_{\rho_c^+, \mathcal{X}_p, \mathcal{Z}_q}(\rho) = (\bar{p}\bar{q}\rho + p\bar{q}X\rho X + \bar{p}qZ\rho Z) \otimes \rho_c^+ + pq(Y\rho Y) \otimes \rho_c^- \quad (6)$$

with  $\rho_c^- \triangleq |-\rangle \langle -|$ . The proof exploits the anti-commute property  $XZ = -ZX = Y$ .

### C. The communication advantage

According to the bottleneck inequality [16], given the composite operation  $\mathcal{Z}_q \circ \mathcal{X}_p$  and let  $C(\cdot)$  be the quantum capacity, the following upper-bound holds [2]:

$$C(\mathcal{Z}_q \circ \mathcal{X}_p) \leq 1 - \max\{H_2(p), H_2(q)\}, \quad (7)$$

where  $H_2(\cdot)$  denotes the binary Shannon entropy. Also, the same inequality holds for  $\mathcal{X}_p \circ \mathcal{Z}_q$ . Indeed, whenever both  $p$

<sup>2</sup>The definition makes use of the Pauli matrices  $\mathbb{I}$ ,  $X$ ,  $Y$ , defined in [17].

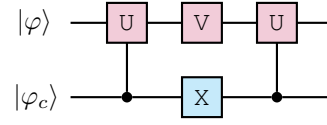


Fig. 1: Quantum circuit implementing a SoCO between unitary operations – with  $|\varphi\rangle$  and  $|\varphi_c\rangle$  denoting the information qubit and the control qubit, respectively.

and  $q$  are set equal to  $\frac{1}{2}$ , we have that both the configurations are characterized by a null capacity, i.e.,  $C(\mathcal{Z}_{\frac{1}{2}} \circ \mathcal{X}_{\frac{1}{2}}) = C(\mathcal{X}_{\frac{1}{2}} \circ \mathcal{Z}_{\frac{1}{2}}) = 0$ .

Let us now consider the two operations combined in a SoCO. Accordingly, with probability  $pq$  the output of equation (6) is given by the second addendum, namely,  $(Y\rho Y) \otimes \rho_c^-$ . As consequence, when both  $p$  and  $q$  are set equal to  $\frac{1}{2}$ , the SoCO capacity is lower-bounded by  $C(\mathcal{S}_{\rho_c^+, \mathcal{X}_{\frac{1}{2}}, \mathcal{Z}_{\frac{1}{2}}}) \geq \frac{1}{4}$ , as shown in [3]. Specifically,  $\rho$  occurs to pass through  $\mathcal{Y}(\rho) = Y\rho Y$ , coherently with control state being  $\rho_c^-$ . Therefore, it is possible to exploit the control state to gain an heralded unitary evolution  $\mathcal{Y}$  via post-selecting evolution with occurrence  $\rho_c^-$ . Since  $\mathcal{Y}$  is unitary, it is also reversible, therefore we can restore the information, gaining a perfect transmission of  $\rho$ , i.e.,  $(\mathcal{Y} \circ \mathcal{Y})(\rho) = Y\rho Y Y = \rho$ . As a visual reminder of what steps are involved within the overall operation, we refer to it as  $\mathcal{S}_{\rho_c^-}$ .

## III. SOCO REALIZATION

In this section we present our steps to realize a SoCO, showing the subject communication advantage.

When the operations are taken to be unitary, say  $\mathcal{U}(\rho) = \mathbb{U}\rho\mathbb{U}^\dagger$  and  $\mathcal{V}(\rho) = \mathbb{V}\rho\mathbb{V}^\dagger$ , the circuit model can directly realize the SoCO operation – circuit in Figure 1 realizes  $\mathcal{S}_{\rho_c, \mathcal{U}, \mathcal{V}}$ . As already mentioned, it is a sub-optimal realization, with a necessary overhead in the query complexity [13].

When considering a SoCO between two non-unitary operations, as in the case of our interest – see equation (6) – the overhead grows up. Indeed, to experience the communication advantage we need to apply a more general circuit.

### A. Realization of non-unitary operations

Mindful of our goal, i.e., realizing a SoCO between operations modeling bit and phase flip channels, we need to generalize the circuit of Figure 1. The circuit model is meant to define algorithms of the type  $\mathbb{U}|\varphi\rangle$ , where  $\mathbb{U}$  is a unitary matrix and  $|\varphi\rangle$  is a quantum state. Instead, the density matrix formalism is more general, and encloses such a kind of operation, equivalently expressed as  $\mathbb{U}|\varphi\rangle \langle \varphi| \mathbb{U}^\dagger$ . However, to involve non-unitary operations, such as the ones of equation (4) and (5), an algorithm  $\mathbb{U}|\varphi\rangle$  cannot work alone and two middle steps are necessary.

Specifically, suppose one wants to realize an operation  $\mathcal{N} : \mathbb{H} \rightarrow \mathbb{H}$  with the circuit model. According to the *Stinespring*

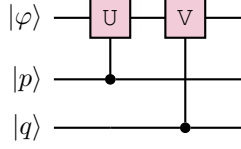


Fig. 2: Quantum circuit realizing the propagation of  $|\varphi\rangle\langle\varphi|$  through  $\mathcal{V}_q \circ \mathcal{U}_p$  operation.

*dilation* [18], one can always associate to  $\mathcal{N}$  a unitary operation  $\mathcal{A}_{\mathcal{N}}$  defined as follows:

$$\mathcal{A}_{\mathcal{N}} : \mathbb{H} \otimes \mathbb{A} \rightarrow \mathbb{H} \otimes \mathbb{A} \quad (8)$$

where  $\mathbb{A}$  is an auxiliary system with associated basis  $\{|a_v\rangle\langle a_w|\}_{vw}$ . Since  $\mathcal{A}_{\mathcal{N}}$  is unitary, it has direct realization with the circuit algorithm.

But our interest is into the realization of  $\mathcal{N}$  operation. To obtain it from  $\mathcal{A}_{\mathcal{N}}$ , one need to *discard* the auxiliary system from  $\mathbb{H} \otimes \mathbb{A}$ . In terms of operations, discarding the auxiliary system means applying a *partial trace*  $\text{Tr}_2 : \mathbb{H} \otimes \mathbb{A} \rightarrow \mathbb{H}$ . Specifically, for a generic state  $\rho_{\mathbb{H} \otimes \mathbb{A}} = \sum_{ijvw} c_{ijvw} (|\varphi_i\rangle\langle\varphi_j| \otimes |a_w\rangle\langle a_v|)$ , the partial trace outputs the following [19]:

$$\text{Tr}_2(\rho_{\mathbb{H} \otimes \mathbb{A}}) = \sum_{ijvw} c_{ijvw} |\varphi_i\rangle\langle\varphi_j| \langle a_w|a_v\rangle. \quad (9)$$

When applying equation (9) to a density matrix  $\rho_{\mathbb{H} \otimes \mathbb{A}}$ , we say that we are tracing out system  $\mathbb{A}$ , getting  $\rho_{\mathbb{H}}$  defined on subsystem  $\mathbb{H}$ . Since  $\mathbb{H}$  and  $\mathbb{A}$  are taken to be generic systems, equation (9) has a direct generalization to the form  $\text{Tr}_{i_1, \dots, i_k}$ , taking as input a density matrix  $\rho_{\mathbb{H}_1 \otimes \dots \otimes \mathbb{H}_n}$  and tracing out subsystems  $\mathbb{H}_{i_1}, \dots, \mathbb{H}_{i_k}$ , with  $k \leq n$ .

In summary, we just outlined a method to realize an operation  $\mathcal{N}$ , involving two steps:

- 1) realizing the circuit  $\mathcal{A}_{\mathcal{N}}$ ;
- 2) discarding the auxiliary system with a partial trace  $\text{Tr}_2$ .

To our purpose, we apply this method, restricted to a more specific class of operations. Namely, given a probability  $p$  and a unitary matrix  $U$ , we define an operation  $\mathcal{U}_p$  as follows:

$$\mathcal{U}_p(\rho) \triangleq (1-p)\mathbb{I}\rho\mathbb{I} + pU\rho U^\dagger. \quad (10)$$

This is general enough to include equation (4) and (5). To realize equation (10) as circuit, we will make use of an extra quantum system (an extra qubit), which has the task of encoding the two probabilities  $p$  and  $1-p$ , i.e.,  $|p\rangle \triangleq \sqrt{1-p}|0\rangle + \sqrt{p}|1\rangle$ . The result is a circuit performing a controlled- $U$  operation with  $|p\rangle$  being the control qubit. The circuit is clearly modular, in the sense that one may compose any two (or more) operations  $\mathcal{U}_p$  and  $\mathcal{V}_q$  from class of equation (10)<sup>3</sup>, to realize a  $\mathcal{V}_q \circ \mathcal{U}_p$  operation - see Figure 2.

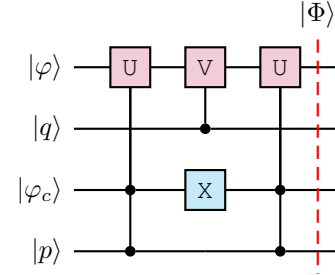


Fig. 3: Circuit implementing a SoCO. The information  $|\varphi\rangle\langle\varphi|$  is subject to a superposition of operations  $\mathcal{V}_q \circ \mathcal{U}_p$  and  $\mathcal{U}_p \circ \mathcal{V}_q$ , coherently with  $|\varphi_c\rangle\langle\varphi_c|$ .

### B. Circuit definition

Starting from the discussion above, it is reasonable to extend the circuit of Figure 1, to realize not only SoCO between unitary operations, i.e., any  $\mathcal{S}_{\rho_c, \mathcal{U}, \mathcal{V}}$ , but a more general form, involving the non-unitary operations of equation (10), i.e.,  $\mathcal{S}_{\rho_c, \mathcal{U}_p, \mathcal{V}_q}$ . The new circuit is shown in Figure 3. First and third wire represent, respectively, the evolution of information and control qubit. The other two wires (second and fourth) act on auxiliary qubits, used to implement  $\mathcal{V}_q$  and  $\mathcal{U}_p$ .

To realize  $\mathcal{S}_{\rho_c, \mathcal{U}_p, \mathcal{V}_q}$  starting from the new circuit in Figure 3, a discarding of auxiliary qubits is necessary, i.e., through the partial trace. More formally, let  $|\Phi\rangle$  be the output global state, as depicted in Figure 3. With some algebraic manipulation it is possible to calculate  $\text{Tr}_{2,4}(|\Phi\rangle\langle\Phi|)$ , corresponding to trace out the evolution of 2-nd and 4-th qubit from the circuit.

We expand the final matrix, restricted to the subject case  $\mathcal{U}_p = \mathcal{X}_{\frac{1}{2}}$ ,  $\mathcal{V}_q = \mathcal{Z}_{\frac{1}{2}}$  and  $|\varphi_c\rangle = |+\rangle$ . By doing some algebraic manipulation, it results the equivalence  $\text{Tr}_{2,4}(|\Phi\rangle\langle\Phi|) = \mathcal{S}_{\rho_c, \mathcal{X}_{\frac{1}{2}}, \mathcal{Z}_{\frac{1}{2}}}(|\varphi\rangle\langle\varphi|)$ . Indeed, by assuming  $|\varphi\rangle = \alpha|0\rangle + \beta|1\rangle$ , both the operations lays to

$$\frac{1}{4} \begin{bmatrix} |\alpha|^2 + |\beta|^2 & |\alpha|^2 & 0 & \beta\alpha^* \\ |\alpha|^2 & |\alpha|^2 + |\beta|^2 & \beta\alpha^* & 0 \\ 0 & \alpha\beta^* & |\alpha|^2 + |\beta|^2 & |\beta|^2 \\ \alpha\beta^* & 0 & |\beta|^2 & |\alpha|^2 + |\beta|^2 \end{bmatrix}. \quad (11)$$

### C. Circuit optimization

It is worth to note that when submitting any circuit to a real processor, a standard practice is mapping it to some new circuit - mathematically equivalent - featuring primitive operations that the physical hardware supplies [20]. The mapping procedure generally induces overhead, due to an increase in the number of operations. This is a problem, since the real processor is affected by decoherence and any extra operation may critically affect the experiments.

Specifically to our proposal - i.e., circuit in Figure 3 - we note that a potentially strong overhead may come from the use of an operation involving 3-qubits, namely, the doubly controlled unitary  $U$  operation. To our purpose - i.e., implementing equation

<sup>3</sup>Coherently with equation (10), given a unitary matrix  $V$  and a probability  $q$ , it follows the equation  $\mathcal{V}_q(\rho) = (1-q)\rho + pV\rho V^\dagger$ .

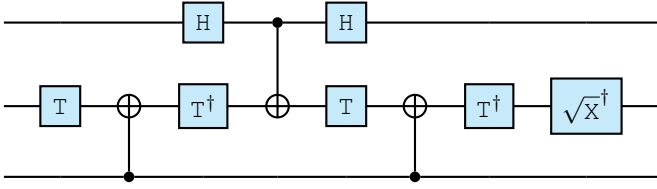


Fig. 4: Whenever the second wire takes  $|+\rangle$  as input, this circuit acts as a Toffoli operation with first qubit being the target. Operations occurring in this circuit are standard; the reader may find a definition in [17].

(6) - we fixed  $U = X$ , corresponding to the well known Toffoli operation. The Toffoli has no direct physical implementation and it has a standard mapping translating it into a sequence of 1-qubit and 2-qubits operations [17]. Fortunately, when the input domain is restricted, an equivalent and less expensive sequence of operations exists. Specifically to our scenario, since the control qubit is fixed to  $|\varphi_c\rangle = |+\rangle$ , the first Toffoli occurring in the circuit of Figure 3 has an optimized mapping to circuit of Figure 4, w.r.t. the standard mapping.

#### IV. EXPERIMENTS

In this section we present an experimental comparison between a SoCO operation, modeling the communication advantage, and one of the two corresponding classically-ordered operations, occurring in that SoCO. Formally speaking, the comparison is between the operations  $\mathcal{S}_{\rho_c^\dagger, \mathcal{X}_{\frac{1}{2}}, \mathcal{Z}_{\frac{1}{2}}}$  and  $\mathcal{Z}_{\frac{1}{2}} \circ \mathcal{X}_{\frac{1}{2}}$ . To this aim, first we show the tools we used for the analysis. After that we report the results of experiments conducted on a superconductor processor, supplied by IBM [11].

The meaning behind such a comparison is experiencing the communication advantage within a NISQ architecture. We also evaluate the overall performance, giving a first insight on the capabilities of NISQ architecture to realize SoCO of non-unitary operations.

##### A. Fidelity measure

To evaluate the performance of our SoCO realization, we made use of the fidelity measure defined accordingly with [21]. Formally, the definition originally comes from the fidelity for mixed-states  $F(\rho_1, \rho_2) = \text{Tr}(\sqrt{\sqrt{\rho_1}\rho_2\sqrt{\rho_1}})^2$  with  $\rho_1$  and  $\rho_2$  being states. However, we can also use that same metrics to evaluate operations.

For a given operation  $\mathcal{N}$  acting on  $d$  degrees of freedom, there exists a matrix  $\Lambda_{\mathcal{N}}$  such that

$$\mathcal{N}(\rho) = \text{Tr}_2((\mathbb{1} \otimes \rho^T)\Lambda_{\mathcal{N}}) \quad (12)$$

Where  $\text{Tr}_2$  is the partial trace defined in equation (9).  $\Lambda_{\mathcal{N}}$  is known as Choi-matrix and it has a one-to-one correspondence with  $\mathcal{N}$ .

Given two operations  $\mathcal{N}$  and  $\tilde{\mathcal{N}}$ , both defined on the same space, authors in [21] showed that  $F(\frac{\Lambda_{\mathcal{N}}}{d}, \frac{\Lambda_{\tilde{\mathcal{N}}}}{d})$  is a fidelity measure. Therefore, we make use of that function to evaluate

how much any two operations differ from each other. For the sake of readability, let us restate the function with the operations as parameters:

$$\text{CF}(\mathcal{N}, \tilde{\mathcal{N}}) = F\left(\frac{\Lambda_{\mathcal{N}}}{d}, \frac{\Lambda_{\tilde{\mathcal{N}}}}{d}\right). \quad (13)$$

From now on, we will refer to function  $\text{CF}$  of equation (13) as the fidelity of two given operations.

##### B. Characterizing operations

An implementation of a circuit executed on some real processor inevitably differs from ideal behaviour, due to noise and imperfections characterizing NISQ architectures.

Formally, running an operation  $\mathcal{N}$ , lays to a new real one, approximating  $\mathcal{N}$ . The way it differs from  $\mathcal{N}$  is generally not known *a priori*, because of the complex time-dependent characteristics of the hardware. Therefore, to evaluate the performance, one need to conduct several experiments. For this reason, we refer to a single experiment  $^{\text{ex}}$  running  $\mathcal{N}$  as  $\mathcal{N}^{\text{ex}}$ , whilst  $\{\mathcal{N}^{\text{ex}}\}$  is a sample of experiments.

As already discussed, any operation  $\mathcal{N}$  is uniquely described by its Choi-matrix  $\Lambda_{\mathcal{N}}$  – see equation (12). To characterize  $\Lambda_{\mathcal{N}}$ , we used a process tomography method, supplied by IBM. All the experiments were shot over the same processor, i.e. `ibmq_santiago`. Thus getting two samples, each of 100 results:  $\{\mathcal{S}_{\rho_c^\dagger}^{\text{ex}}\}$  and  $\{(\mathcal{Z}_{\frac{1}{2}} \circ \mathcal{X}_{\frac{1}{2}})^{\text{ex}}\}$ .

##### C. Verification of the communication advantage

Here, we experimentally verify that  $\mathcal{S}_{\rho_c^\dagger}$  gives an advantage over  $\mathcal{Z}_{\frac{1}{2}} \circ \mathcal{X}_{\frac{1}{2}}$ , from a communication perspective. Coherently with previous discussion, we acquired samples  $\{\mathcal{S}_{\rho_c^\dagger}^{\text{ex}}\}$  and  $\{(\mathcal{Z}_{\frac{1}{2}} \circ \mathcal{X}_{\frac{1}{2}})^{\text{ex}}\}$ .

We exploit fidelity measure defined in (13) to quantify the advantage. Specifically, we evaluate how  $\{\mathcal{S}_{\rho_c^\dagger}^{\text{ex}}\}$  and  $\{(\mathcal{Z}_{\frac{1}{2}} \circ \mathcal{X}_{\frac{1}{2}})^{\text{ex}}\}$  differ from a perfect communication channel, modeled by the identity operation  $\mathcal{I}(\rho) = \mathbb{I}\rho\mathbb{I} = \rho$ . The result is two new samples  $\{\text{CF}(\mathcal{I}, \mathcal{S}_{\rho_c^\dagger}^{\text{ex}})\}$  and  $\{\text{CF}(\mathcal{I}, (\mathcal{Z}_{\frac{1}{2}} \circ \mathcal{X}_{\frac{1}{2}})^{\text{ex}})\}$ . In Figure 5 there is the plot of experimental and fitted Cumulative Distribution Function (CDF) of those samples.

Results shown in Figure 5 are coherent to expectation also in a statistical sense. Indeed, fidelities of sample  $\{\mathcal{S}_{\rho_c^\dagger}^{\text{ex}}\}$  lays within interval  $[0.45, 0.75]$ ; whereas sample  $\{(\mathcal{Z}_{\frac{1}{2}} \circ \mathcal{X}_{\frac{1}{2}})^{\text{ex}}\}$  lays within interval  $[0.2, 0.35]$ . The fact that the two intervals do not intersect highlights the clear-cut advantage.

To further visualize the communication advantage, it is interesting to observe a plot of the noise produced by running  $\mathcal{S}_{\rho_c^\dagger}$  and  $\mathcal{Z}_{\frac{1}{2}} \circ \mathcal{X}_{\frac{1}{2}}$  for two high-fidelity experiments. Since both the operations model the transformation over a single qubit, we can plot them as a deformation of the corresponding bloch spheres - see Figure 6. The plots stand out our result. In Figure 6a the output sphere keeps a good level of coherence. On contrary, the output sphere of Figure 6b has a high information loss, represented by the collapse of the sphere to the center.

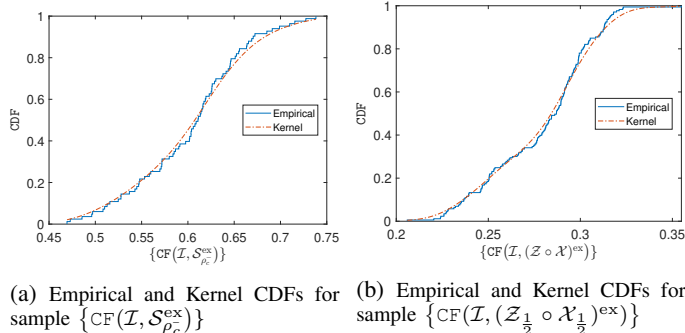


Fig. 5: Either figure (a) or (b) shows the performance - i.e., CDF of fidelities - of the processor running a given circuit. The blue solid line is the empirical CDF - computed with the MATLAB `ecdf` method. Whereas, the red dashed line is the Kernel distribution -- computed with the MATLAB `ksdensity` method - derived from the empirical CDF.

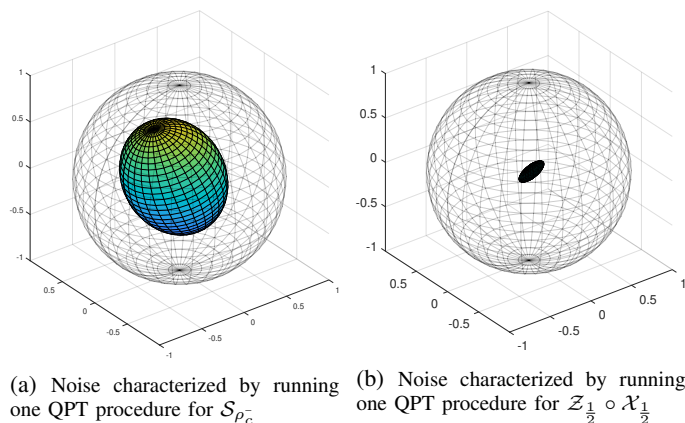


Fig. 6: Bloch sphere representation of the two characterized operations. Grey sphere represents the ideal sphere, corresponding to a set of pure states. The inside coloured sphere is the deformation induced by the circuit.

## V. CONCLUSIONS

In this paper we addressed the SoCO and its realization within a programmable superconductor processor, based on the standard quantum circuit model. Before this paper, there was no experimental evaluation of the SoCO in a NISQ architecture, especially between non-unitary operations. NISQ architectures are widespread technologies, likely to rapidly evolve. It is therefore of crucial importance to evaluate the SoCO as possible resources. As a first insight in this direction, we gave a comparison, to experience and evaluate a SoCO operation, presenting promising phenomena from a communication perspective, i.e., achieving information transmission through null-capacity channels.

## REFERENCES

[1] D. Ebler, S. Salek, and G. Chiribella, "Enhanced communication with the assistance of indefinite causal order," *Physical review letters*, vol. 120, no. 12, p. 120502, 2018.  
 [2] S. Salek, D. Ebler, and G. Chiribella, "Quantum communication in a superposition of causal orders." *arXiv preprint arXiv:1809.06655*, 2018.

[3] M. Caleffi and A. S. Cacciapuoti, "Quantum Switch for the Quantum Internet: Noiseless Communications through Noisy Channels." *IEEE Journal on Selected Areas in Communications*, vol. 38, no. 3, pp. 575–588, 2020.  
 [4] G. Chiribella, "Perfect discrimination of no-signalling channels via quantum superposition of causal structures." *Physical Review A*, vol. 86, no. 4, p. 040301, 2012.  
 [5] M. Araújo, F. Costa, and Č. Brukner, "Computational advantage from quantum-controlled ordering of gates." *Physical Review Letters*, vol. 113, no. 25, p. 250402, 2014.  
 [6] L. M. Procopio, A. Moqanaki, M. Araújo *et al.*, "Experimental superposition of orders of quantum gates." *Nature Communications*, vol. 6, no. 1, pp. 1–6, 2015.  
 [7] G. Rubino, L. A. Rozema, A. Feix, M. Araújo, J. M. Zeuner, L. M. Procopio, Č. Brukner, and P. Walther, "Experimental verification of an indefinite causal order." *Science Advances*, vol. 3, no. 3, p. e1602589, 2017.  
 [8] Y. Guo, X.-M. Hu, Z.-B. Hou, H. Cao, J.-M. Cui, B.-H. Liu, Y.-F. Huang, C.-F. Li, G.-C. Guo, and G. Chiribella, "Experimental transmission of quantum information using a superposition of causal orders," *Physical Review Letters*, vol. 124, no. 3, p. 030502, 2020.  
 [9] J. F. Fitzsimons, J. A. Jones, and V. Vedral, "Quantum correlations which imply causation." *Scientific Reports*, vol. 5, no. 1, pp. 1–7, 2015.  
 [10] K. Goswami, C. Giarmatzi, M. Kewming, F. Costa, C. Branciard, J. Romero, and A. G. White, "Indefinite causal order in a quantum switch," *Physical Review Letters*, vol. 121, no. 9, p. 090503, 2018.  
 [11] "IBM Quantum," <https://quantum-computing.ibm.com/>, 2021.  
 [12] D. Castelvecchi, "IBM's Quantum Cloud Computer goes Commercial." *Nature*, vol. 543, no. 7644, p. 159, Mar. 2017.  
 [13] G. Chiribella, G. M. D'Ariano, P. Perinotti, and B. Valiron, "Quantum computations without definite causal structure." *Physical Review A*, vol. 88, no. 2, p. 022318, 2013.  
 [14] D. Deutsch, "Quantum theory, the church-turing principle and the universal quantum computer." *Proceedings of the Royal Society of London A: Mathematical, Physical and Engineering Sciences*, vol. 400, pp. 97–117, 1985.  
 [15] J. Preskill, "Quantum Computing in the NISQ era and beyond." *Quantum*, vol. 2, no. 79, 2018.  
 [16] M. M. Wilde, *Quantum Information Theory*. Cambridge University Press, 2013.  
 [17] M. A. Nielsen and I. L. Chuang, *Quantum Computation and Quantum Information*. Cambridge University Press, 2010.  
 [18] W. F. Stinespring, "Positive functions on C\*-algebras," *Proceedings of the American Mathematical Society*, vol. 6, no. 2, pp. 211–216, 1955.  
 [19] E. G. Rieffel and W. H. Polak, *Quantum computing: A gentle introduction*. MIT Press, 2011.  
 [20] D. Cuomo, M. Caleffi, and A. S. Cacciapuoti, "Towards a distributed quantum computing ecosystem." *IET Quantum Communication*, vol. 1, pp. 3–8, July 2020, Invited Paper.  
 [21] M. Raginsky, "A fidelity measure for quantum channels." *Physics Letters A*, vol. 290, no. 1-2, pp. 11–18, 2001.